J. Electroanal. Chem., 255 (1988) 199–213
Elsevier Sequoia S.A., Lausanne – Printed in The Netherlands

The influence of the halide electrolyte on the electrochemical reduction pathway of some *meso*-tetrasubstituted porphyrin free bases in *N,N*-dimethyl formamide

Christopher M.A. Brett and Ana Maria C.F. Oliveira Brett

Departamento de Química, Universidade de Coimbra, 3049 Coimbra (Portugal)

(Received 3 May 1988; in revised form 29 June 1988)

ABSTRACT

Differential pulse, cyclic and rotating disc voltammetry have been used to study the redox properties of *meso*-tetra-n-propylporphyrin (TPrP), *meso*-tetramethylporphyrin (TMP) and *meso*-tetraphenylporphyrin (TPP) at glassy carbon electrodes in tetraalkylammonium electrolyte in *N,N*-dimethyl formamide solvent.

Electrochemical reduction of the porphyrins is affected by the electrolyte employed. There is a large influence from the electrolyte anion and only a small one from the cation, shown by the difference in half-wave reduction potentials between tetrabutylammonium and tetraethylammonium electrolytes, both effects independent of the electrode material being glassy carbon or mercury. A systematic study on the influence of the anion was undertaken using TPrP and TPP in halide (chloride, bromide and iodide) salts of tetrabutylammonium electrolytes, including variation of the quantity of halide ion present, the behaviour in 0.1 *M* tetrabutylammonium perchlorate being taken as the reference. Trends in half-wave potential and wave shape from chloride to perchlorate are more accentuated for TPrP than for TPP. UV–visible spectra of the porphyrins were found to be electrolyte invariant. Rationalisation in terms of interaction between the porphyrin mononegative ion and the halide ion providing an alternative, anion concentration dependent, reduction pathway is discussed.

INTRODUCTION

The large amount of research into porphyrin electrochemistry was initially directed towards the elucidation of the role played by porphyrin containing molecules in the biological electron transfer chain [1–3]. More recently applications of a widespread nature have been proposed, such as adsorbed electrocatalysts [4,5], in modification of electrode surfaces [6,7], and as an integral ingredient for composite electrodes [8].

In natural systems the porphyrin ring nearly always contains a central metal cation. Investigations have shown that the electrochemistry of metalloporphyrins is,

0022-0728/88/$03.50

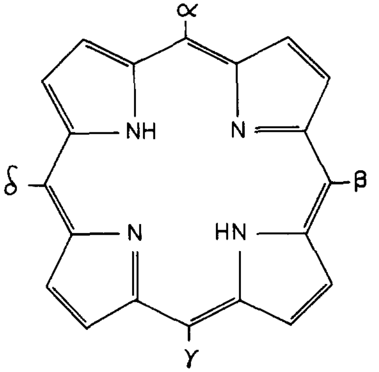

Fig. 1. The porphyrin molecule, showing the positions for *meso* substitution (α, β, γ, δ).

to a good approximation, a superposition of the effect of the ring structure and the effect of the central metal cation, which can be confirmed by relatively simple Hückel-type calculations [9–12]. Studies of porphyrin free bases are thus important and useful in clarifying the role of the central metal cation. A large number of these free bases have been investigated with respect to their electrochemical reduction, principally at mercury owing to its large negative potential range, and conclusions drawn with respect to ring substituent effects on electrochemical behaviour [13,14]. It has been noted that, as for many organic compounds, there is a dependence on electrode material, solvent, and added electrolyte [1,2]. Some oxidation studies have been done at platinum electrodes [10,15].

We have been studying the redox properties of *meso*-tetraalkyl- and *meso*-tetraphenylporphyrin free bases (Fig. 1) in *N*,*N*-dimethyl formamide (DMF) at glassy carbon electrodes (potential range in DMF −2.7 to +0.7 V vs. SCE). The production of *meso*-tetraalkylporphyrins in reasonable yield, and without chlorin contamination, is now possible owing to modifications to the classical Rothemund synthesis [16]: purification is thus easier to perform and electrochemical studies are facilitated. Comparisons are made between alkyl and phenyl substituted free bases, using cyclic, rotating disc and differential pulse voltammetry, and an investigation made into the role of the supporting electrolyte on electrochemical reduction.

EXPERIMENTAL

The porphyrins used were *meso*-tetra-n-propylporphyrin (TPrP), *meso*-tetramethylporphyrin (TMP) and *meso*-tetraphenylporphyrin (TPP) and were a gift from Prof. A. d'A. Rocha Gonçalves. They were carefully purified by recrystallisation and stored in the dark. Supporting electrolytes employed were the chloride, bromide, iodide and perchlorate salts of tetrabutylammonium (TBAC, TBAB, TBAI and TBAP respectively), and tetraethylammonium bromide (TEAB), obtained from Fluka AG as purissimum (purum in the case of TBAC); they were treated by standard purification procedures before use [17]. *N,N*-dimethyl formamide (DMF) solvent (Merck pro analysi) was dried with calcium oxide and sodium hydroxide for 24 h, distilled at reduced pressure under nitrogen and stored over Linde 4A molecular sieves in the dark, being utilised within a maximum of two days of distillation. Its purity, initially checked chromatographically, was routinely checked before each experiment by running supporting electrolyte voltammograms, which gave a good indication of the presence of impurities or degradation products; on evidence of any abnormal behaviour the DMF was rejected and fresh solvent prepared.

A glassy carbon (Plessey) rotating disc electrode (RDE), of radius 0.35 cm, with Kel-F sheath was used for rotating disc voltammetry experiments, and for cyclic and differential pulse voltammetry at zero rotation speed. After initial polishing down to 1 μm with diamond lapping compound (Hyprex Diamond Spray, Engis) on a polishing table, 0.3 μm highly pure polishing alumina (BDH Chemicals Ltd.) was used before each experiment, and between recording of successive voltammograms unless otherwise specified. The electrode was then cleaned thoroughly in triply distilled water, carefully dried with paper tissue and washed in DMF solvent before being introduced into the cell. The cell, painted black to avoid any photochemical reaction, was thermostatted at $25.0 \pm 0.1°$ C using a Haake G circulation thermostat bath, by means of a surrounding water jacket. Besides the working electrode, the cell also contained a platinum gauze auxiliary electrode and a Radiometer K401 saturated calomel reference electrode. The frit of this electrode is sufficiently resistant to solution movement over the timescale of the experiment that no problems were encountered with destruction of the reference electrode due to disproportionation of Hg(I), as described by Mann [18].

The mercury plated glassy carbon electrode was prepared by mercury deposition, whilst rotating the electrode at 4 Hz, from a solution containing 10^{-5} *M* Hg(II) in 0.4 *M* K_2SO_4 by application of a potential of -0.3 V for 5 min; the electrode was then washed several times with DMF before use. The hanging mercury drop electrode (HMDE) (Metrohm E410) was used with triply distilled mercury.

The rotating assembly (Oxford Electrodes) was linked to a home-made potentiostat of standard construction [19]. Differential pulse voltammetry experiments were performed with a PAR 174A polarographic analyser; the pulse amplitude was 50 mV and the period between pulses was 0.5 s. Voltammograms were registered on a HP 7035B X–Y recorder and potentials measured with a Fluke 8050A digital multimeter. All connections were made with screened leads.

Deoxygenation was performed with U-grade (ultra pure oxy-free) nitrogen (Ar Líquido), passed over silica gel and calcium oxide to remove residual water and through DMF solvent before being introduced into the cell. Bubbling was done for at least 30 min at the beginning of each experiment, making sure that the oxygen reduction wave disappeared totally [20]. Between recording of voltammograms, after cleaning the electrode, about 5 min bubbling was necessary. During recording, nitrogen was introduced into the cell above the solution.

UV–visible spectra were recorded on a Hitachi 220S spectrophotometer.

RESULTS

The redox behaviour of porphyrin free bases may be characterised conveniently by the first two reductions. Representing the free base as H_2P, they can be written:

$$H_2P + e^- \rightarrow H_2P^{\cdot -} \qquad E_{1/2}(1)$$

$$H_2P^{\cdot -} + e^- \rightarrow H_2P^{2-} \qquad E_{1/2}(2)$$

The added electrons are accommodated in π molecular orbitals. ESR studies have confirmed reduction to the dianion [11]. Further reduction steps involve proton abstraction from the solvent [12].

Voltammetric behaviour in TBAP

In Fig. 2 and Tables 1 and 2 are shown typical results obtained in 0.1 *M* TBAP electrolyte for the porphyrins TMP, TPrP and TPP using cyclic and rotating disc voltammetry. The peak separation between forward and backward scans for the first two reduction steps is invariant with sweep rate at ≈ 60 mV in the cyclic voltammo-

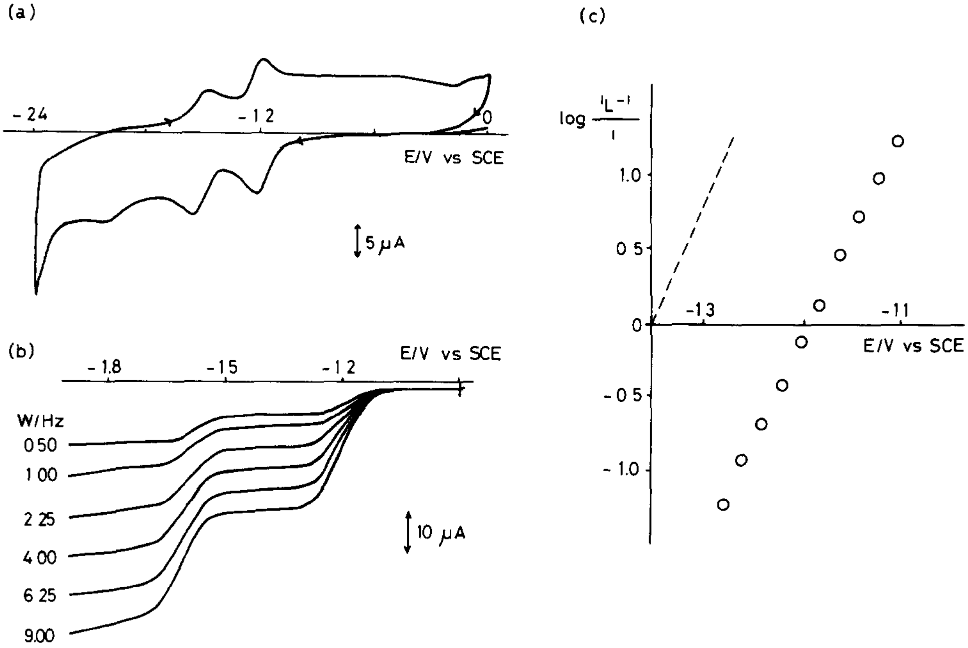

Fig. 2. Typical reduction behaviour of *meso*-tetraalkyl porphyrin in 0.1 *M* TBAP+DMF at GCE, illustrated for TMP (3.1×10^{-4} *M*). (a) Cyclic voltammogram (scan rate 100 mV s^{-1}). (b) Rotating disc voltammograms. (c) Tafel-type plot of first reduction wave taken from Fig. 2b with $W = 9$ Hz; dotted line has slope (1/59) mV^{-1}.

TABLE 1

Reversible reduction half-wave potentials vs. SCE in 0.1 *M* tetrabutylammonium electrolytes at glassy carbon electrodes in DMF [a]. Data from cyclic and RDE voltammograms. Solution contains $\approx 5 \times 10^{-4}$ *M* porphyrin. $\Delta E = E_{1/2}(1) - E_{1/2}(2)$

Porphyrin	Electrolyte	$E_{1/2}(1)$/V	$E_{1/2}(2)$/V	ΔE/V
TPP	TBAP	−1.06	−1.50	0.44
	TBAI	−1.08	−1.53	0.45
	TBAB	−1.03	−1.46	0.43
	TEAB	−1.02	−1.43	0.41
TPrP	TBAP	−1.23	−1.65	0.42
	TBAI	−1.24	−1.66	0.42
	TBAB	−1.23	−1.64	0.41
	TEAB	−1.22	−1.55	0.33
TMP	TBAP	−1.19	−1.58	0.39
	TEAB	−1.22	−1.55	0.33

[a] Reduction waves not reversible in TBAC electrolyte (see text and figures).

grams. At the RDE we obtain linear plots of $\log[(i_L - i)/i]$ vs. E (Fig. 2c) and constant values of $E_{1/2}$, independent of rotation speed. We can thus conclude that the two one-electron reductions are reversible, as found previously at mercury electrodes [9]. The smaller peak at ≈ -2.0 V is obtained in the absence of porphyrin in pure supporting electrolyte.

There are several points worth noting. Firstly, from Table 1, it is clear that TPP is reduced more easily than the *meso*-tetraalkylporphyrins, attributable to the phenyl substituent allowing extra delocalisation of the π electrons in the conjugated cyclic system. The first two reduction potentials of porphin, the parent unsubstituted porphyrin, of −1.19 and −1.61 V vs. SCE [13] are almost identical to those of the *meso*-tetraalkylporphyrins, showing the very small effect of alkyl groups on electron charge distribution.

TABLE 2

Diffusion coefficient values at glassy carbon RDE for $\approx 5 \times 10^{-4}$ *M* porphyrin in 0.1 *M* electrolyte + DMF, calculated from plot of limiting current vs. (rotation speed)$^{1/2}$, for reduction to anion radical ($n = 1$), and dianion ($n = 2$). Electrode cleaned between scans

Electrolyte	$10^5\ D/\text{cm}^2\ \text{s}^{-1}$					
	TPP		TPrP		TMP	
	$\text{TPP}^{\cdot -}$	TPP^{2-}	$\text{TPrP}^{\cdot -}$	TPrP^{2-}	$\text{TMP}^{\cdot -}$	TMP^{2-}
TBAP	0.69	0.69	0.67	0.67	0.42	0.42
TBAI	0.69	0.69	0.68	0.67	–	–
TBAB	0.53	0.38	0.47	0.35	–	–
TBAC	0.47	–	0.53	–	–	–
TEAB	0.55	0.38	0.46	0.35	0.38	0.31

Secondly, the nearly constant difference between $E_{1/2}(1)$ and $E_{1/2}(2)$ at around 400 mV. This has been noted in previous studies for a wide range of porphyrins with and without central metal ions: according to Clack and Hush [9], it means that the solvation energies of the mononegative ions are more or less equal. We have also observed for these porphyrins, at glassy carbon, that the difference between the first oxidation potential and the first reduction potential is around 2.05 V, confirming that the substituents have similar effects on the LUMO and HOMO [3]. However, unlike most cases described in the literature [10,15], we saw a single two-electron oxidation wave, rather than two one-electron waves.

Thirdly, the diffusion coefficient values (Table 2), calculated from RDE plots of i_L vs $W^{1/2}$ via the well-known expression:

$$i_L = 1.554 nF\pi r^2 D^{2/3} \nu^{-1/6} C_\infty W^{1/2}$$

where r is the electrode radius, c_∞ the concentration of electroactive species, W the rotation speed in Hz, and all other symbols have their usual meaning. Whereas the diffusion coefficients for TPrP and TPP are almost equal, that of TMP is significantly smaller. This rather unexpected result may be due to some form of association of species in the latter case, this being impeded sterically by the larger size of the *meso* substituents in TPrP and TPP.

Reduction of TPrP and TPP in different tetraalkylammonium halide electrolytes

The electrochemical behaviour described above undergoes a number of important modifications when we change the supporting electrolyte. This first came to light when we carried out an experiment using some TEAB available in the laboratory. Following this we investigated the effect of electrolyte anion (iodide, bromide or chloride vs. perchlorate) systematically with tetrabutylammonium cation, electrolyte cation (tetrabutylammonium and tetraethylammonium) and electrode material (glassy carbon or mercury).

Table 1 lists the half-wave reduction potentials for TPrP and TPP in the various electrolytes and Table 2 diffusion coefficients obtained from RDE experiments. Figures 3–8 show cyclic, RDE and differential pulse voltammograms.

Effect of electrolyte anion: 0.1 M iodide vs. 0.1 M perchlorate

The voltammograms in iodide are very similar to those obtained in perchlorate media, and calculated diffusion coefficients are virtually identical.

Effect of electrolyte anion: 0.1 M bromide vs. 0.1 M perchlorate

In bromide electrolyte what appears to be a pre-wave was recorded about 60 mV before the first main reduction wave in the cyclic voltammograms of both porphyrins, disappearing on the second cycle. If the potential scan is reversed after the first reduction then successive scans superimpose on one another. Rotating disc voltammetry showed the pre-wave to be rotation speed dependent (illustrated in Fig. 3 for TPP in TBAB), at low rotation speed (1 Hz), the composite nature of the first

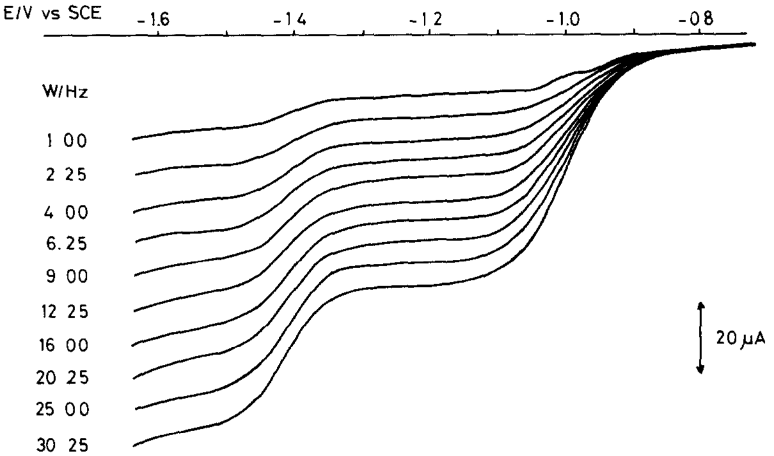

Fig. 3. Rotating disc voltammograms of TPP (3.1×10^{-4} M) in 0.1 M TBAB+DMF at GCE: first and second reduction waves.

reduction wave being immediately obvious. This was confirmed in differential pulse measurements (see later).

Diffusion coefficients (Table 2) are reduced from the TBAP values, more so for reduction to the dianion H_2P^{2-}; half-wave potentials are only slightly altered. Also there is a greater change with respect to perchlorate for TPrP than for TPP.

Effect of electrolyte anion: 0.1 M chloride vs. 0.1 M perchlorate

The cyclic voltammograms in chloride electrolyte show irreversibility in the first and second reduction waves and evidence of adsorption (Fig. 4). In the RDE

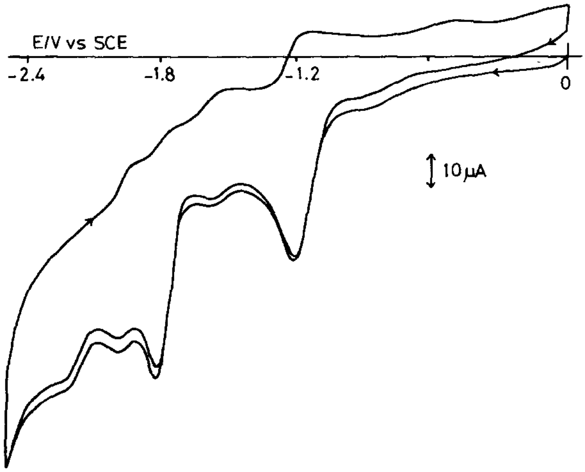

Fig. 4. Cyclic voltammogram of TPrP (5.19×10^{-4} M) in 0.1 M TBAC+DMF at GCE. Scan rate 100 mV s^{-1}.

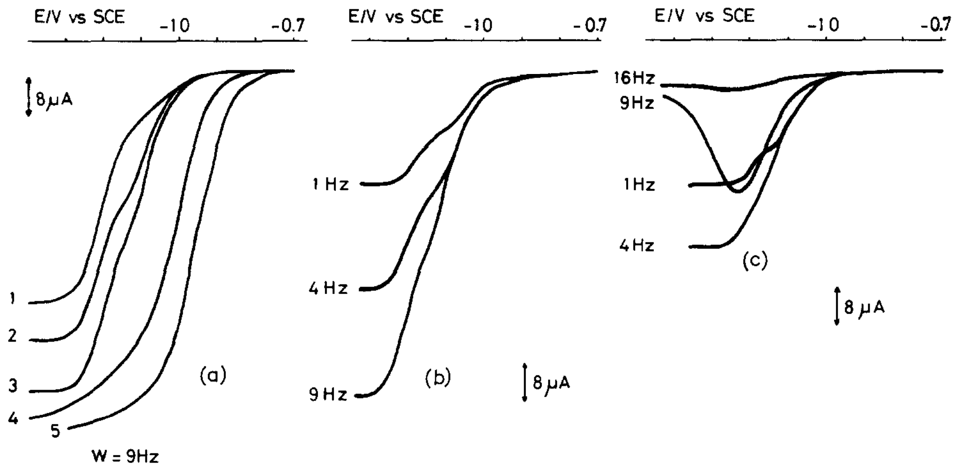

Fig. 5. Rotating disc voltammograms for first reduction wave of TPrP (5.52×10^{-4} *M*) in 0.1 *M* TBAP and with various concentrations of TBAC. (a) Increasing TBAC concentration: (1) [TBAC] = 0; (2) [TBAC] = 5.70×10^{-3}; (3) [TBAC] = 1.14×10^{-2}; (4) [TBAC] = 3.2×10^{-2}; (5) [TBAC] = 5.6×10^{-2} *M*. (b) [TBAC] = 1.13×10^{-2} *M*. Electrode cleaned between each scan. (c) [TBAC] = 1.13×10^{-2} *M*. Electrode not cleaned between scans; scans recorded in order of increasing rotation speed.

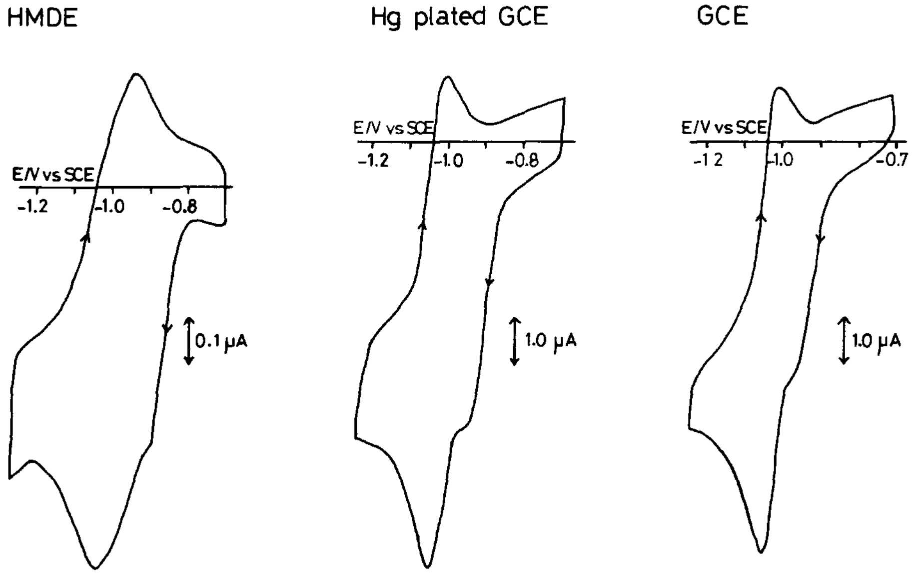

Fig. 6. Cyclic voltammograms for the reduction of TPP (3.2×10^{-4} *M*) in 0.1 *M* TBAB + DMF at HMDE, Hg plated GCE and GCE. Scan rate 20 mV s^{-1}.

voltammograms we see blocking of the electrode surface occurring at higher rotation speeds, causing the current to diminish to a lower, nearly zero, value. The extent to which this occurs depends on the history of the electrode after cleaning, as shown in Figs. 5b and c. The RDE half-wave potential for the first reduction is shifted significantly to more positive potentials with respect to perchlorate; in relation to the diffusion coefficients we note that the value for TPrP is higher than TPP, but less than in TBAP electrolyte. However, see discussion below, we may be looking at a different electrode reaction mechanism.

Effect of the electrolyte cation: tetraethyl- vs. tetrabutylammonium

Inspection of Table 1 shows that $E_{1/2}(1)$ is not altered significantly on changing the electrolyte cation. There is only a slight change in the value of ΔE on using

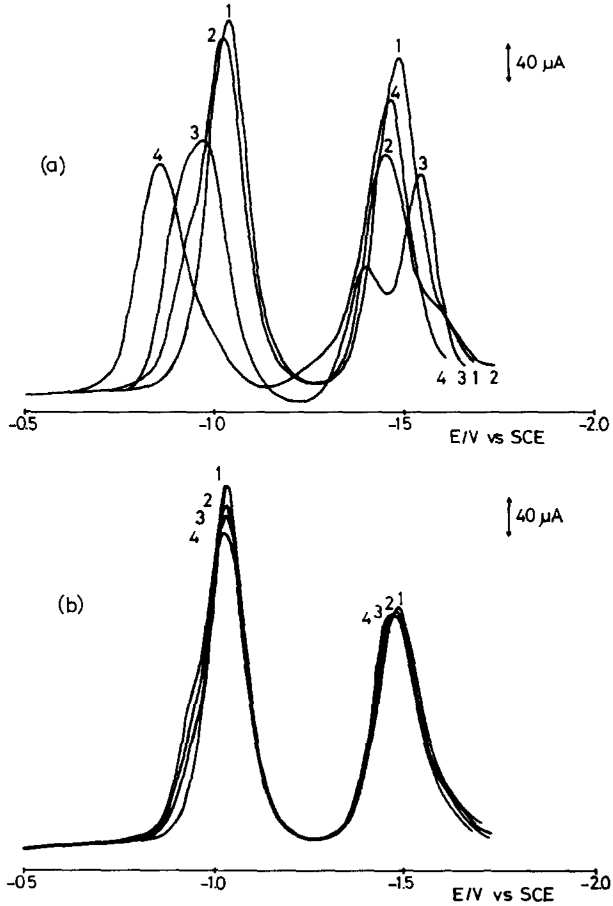

Fig. 7. Differential pulse voltammograms of TPP in TBAC and TBAB containing electrolytes at GCE. [TPP] = 5.9×10^{-4} M; [TBAP] = 0.1 M to which TBAC or TBAB added. Electrode cleaned between scans. (a) TBAC concentration: (1) 0; (2) 1.09×10^{-2}; (3) 4.13×10^{-2}; (4) 6.18×10^{-2} M. (b) TBAB concentration: (1) 0; (2) 9.39×10^{-3}; (3) 3.58×10^{-2}; (4) 8.74×10^{-2} M.

tetraethyl rather than tetrabutylammonium salt. The shape of cyclic and RDE voltammograms is very similar.

Effect of electrode material

The same voltammetric experiments described above were conducted at a mercury plated glassy carbon electrode and at an HMDE; the reason for the use of the HMDE was to check if there was any effect from the tendency of mercury to form tiny droplets on the surface of glassy carbon [21]. No differences due to use of mercury on glassy carbon electrode material were found, illustrated by the cyclic voltammograms in bromide electrolyte (Fig. 6). The slight increase in separation of

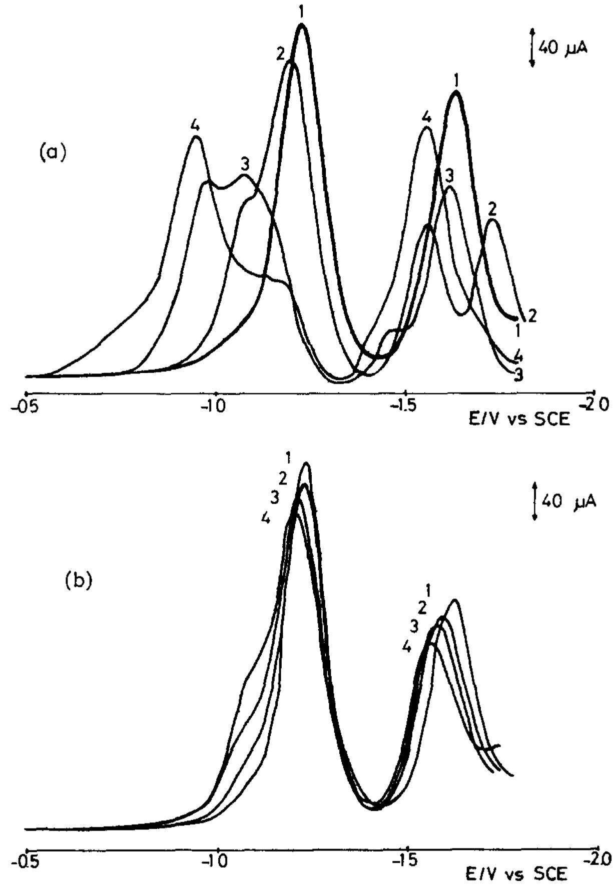

Fig. 8. Differential pulse voltammograms of TPrP in TBAC and TBAB containing electrolytes at GCE. [TPrP] = 5.5×10^{-4} *M*; [TBAP] = 0.1 *M* to which TBAC or TBAB added. Electrode cleaned between scans. (a) TBAC concentration: (1) 0; (2) 3.24×10^{-2}; (3) 5.60×10^{-2}; (4) 1.02×10^{-1} *M*. (b) TBAB concentration: (1) 0; (2) 4.41×10^{-2}; (3) 7.86×10^{-2}; (4) 1.66×10^{-1} *M*.

anodic and cathodic peaks at the HMDE could be due to diffusion of the reduced species to inside the mercury droplet.

Effect of variation of TBAB and TBAC electrolyte concentrations

Two series of experiments were undertaken. In one, the total supporting electrolyte concentration was kept constant at 0.1 *M*, and the quantity of TBAB or TBAC varied from 10^{-3} up to 10^{-1} *M*, the rest being TBAP. In the other, successive quantities of TBAB or TBAC were added to a solution containing the porphyrin and 0.1 *M* TBAP; the concentration of TBAB or TBAC was once more varied from 10^{-3} to 10^{-1} *M*. Experiments were not conducted with TBAI, since it had not shown any significant deviation from TBAP. Results from the two sets of experiments were identical.

We used cyclic, rotating disc and differential pulse voltammetry. The last of these techniques shows most clearly the changes that are occurring, and we focus on these results.

Figures 7 and 8 show some of the DP voltammograms obtained for TPP and TPrP, respectively. For reduction to the mononegative ion, a shoulder correspond-

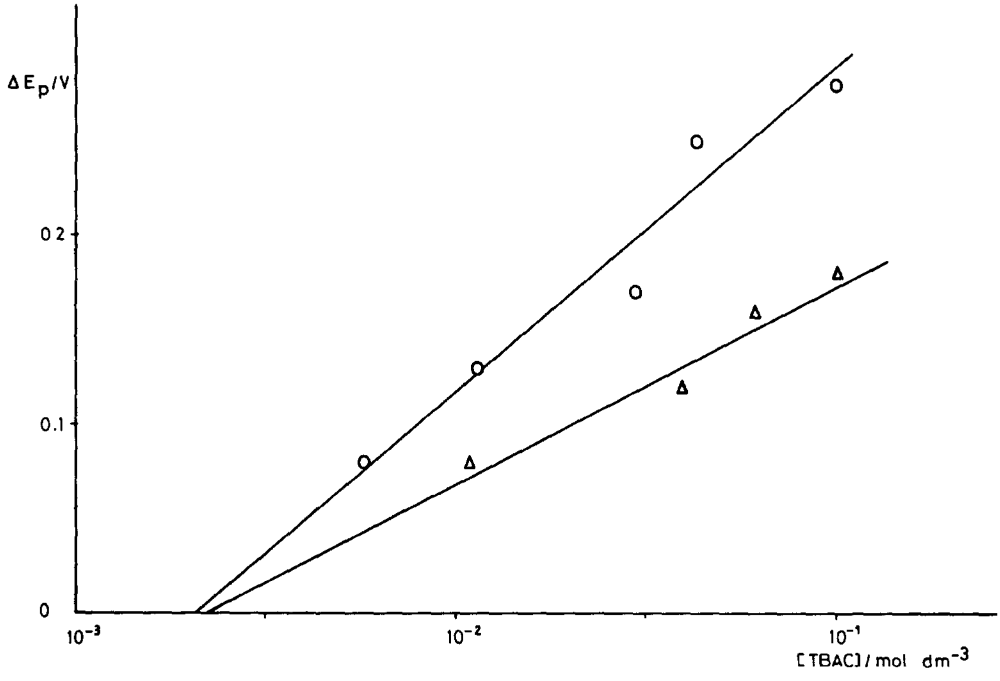

Fig. 9. Plot of variation of peak potential, E_p, of pre-wave with increasing concentration of TBAC in relation to the value for the first reduction of the porphyrin in TBAP, from differential pulse voltammograms, where $\Delta E_p = \{E_p - E_p(\text{TBAP})\}$. (△) TPP; (○) TPrP. E_p(TBAP) values: TPP = −1.06; TPrP = −1.22 V vs. SCE.

ing to the pre-wave begins to appear at fairly low concentrations of TBAC ($\approx 4 \times 10^{-3}$ *M* for TPrP and $\approx 6 \times 10^{-3}$ *M* for TPP); this less negative peak grows in size with increasing chloride concentration, the other decreasing, and shifts towards more positive potentials. Figure 9 shows this variation, which is more accentuated for TPrP, and can be described to a good approximation by a linear variation of E_p with log[TBAC] above a minimum concentration of TBAC of around 2×10^{-3} *M*. In TBAB electrolyte a higher halide concentration is needed to have any effect.

RDE voltammograms alter their form and position with increasing chloride concentration, shown in Fig. 5a, in agreement with the DP results. As described previously, there is evidence of irreversible adsorption occurring.

UV and visible spectra

In Fig. 10 we see the spectra of TPrP and TPP, which are exactly the same in TBAP, TBAI, TBAB and TBAC electrolytes and in the pure solvent. Table 3 lists the peak wavelengths and molar absorption coefficients above the Soret band centred at ≈ 420 nm. Porphyrin spectra are well characterised and all the absorptions are assigned to the conjugated π system. TPrP is red-shifted with respect to

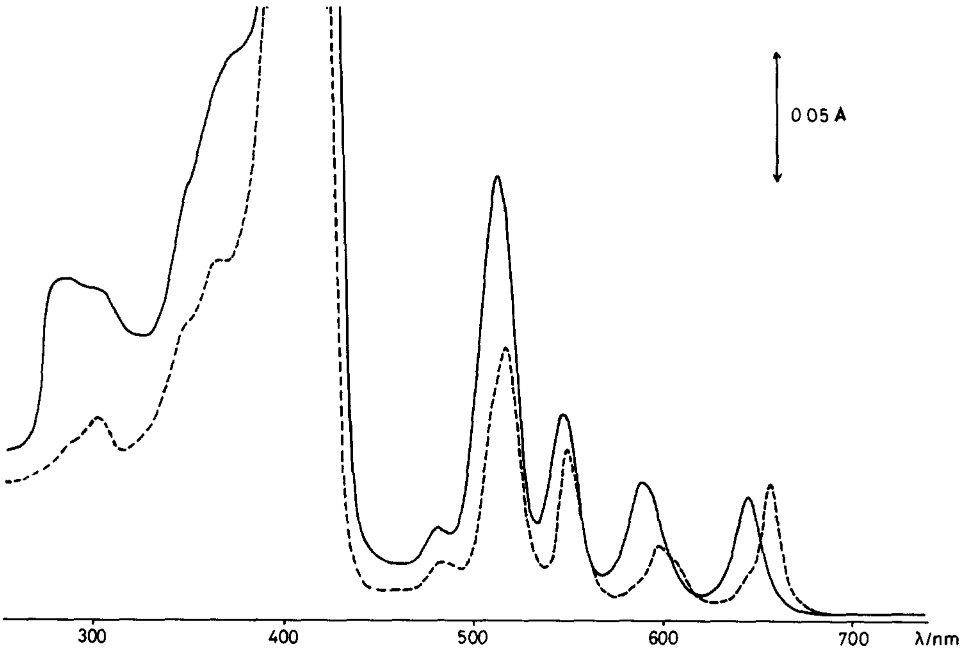

Fig. 10. Spectra of TPP (———) and TPrP (— — —) in the visible region. $[H_2P] = 1.2 \times 10^{-4}$ *M*; 0.1 *M* electrolyte in DMF solvent; path length 0.1 cm. Spectra are invariant with TBAC, TBAB, TBAI, TBAP electrolytes or in pure DMF solvent.

TABLE 3

UV–visible spectra of TPrP and TPP. Peak wavelengths and molar absorption coefficients for peaks above Soret band

TPrP		TPP	
λ_{max}/nm	$10^3\ \epsilon/M\ cm^{-1}$	λ_{max}/nm	$10^3\ \epsilon/M\ cm^{-1}$
482	2.1	480	3.2
517	10.3	514	16.2
550	6.2	548	7.8
597	2.7	590	4.8
656	5.1	646	4.5

TPP and shows slightly different ϵ values. We conclude that there is no strong interaction between the electrolyte and the π system of the neutral molecule.

DISCUSSION

The results presented above show the marked influence of the supporting electrolyte anion on porphyrin reduction, greatest for chloride, less for bromide and none from iodide with respect to perchlorate. Differential pulse results for chloride containing electrolyte are particularly elucidative (Fig. 9); $E_p(2)$ is also affected, but to a smaller extent. UV and visible spectra show that the anion has no effect on the porphyrin ring in H_2P: thus we would expect changes in $E_{1/2}(1)$ or $E_p(1)$ to reflect differences in the energy of $H_2P^{\cdot-}$.

The fact that the smallest anion has the greatest effect suggests a size factor and that it would be useful to consider the dimensions of the porphyrin ring. The radius of the central aperture in the porphyrin monomer is $\approx$ 0.20 nm [22]; crystal radii for the halide anions are: Cl^- 0.181 nm, Br^- 0.196 nm and I^- 0.220 nm [23]. It has also been shown that there is a low energy barrier for deviations in porphyrin conformation from the normal near-planar structure [22]. Furthermore, porphyrin diacid species have been characterised with the halide ion just outside the plane of the porphyrin macrocycle [24]. Interaction between the porphyrin macrocycle and the desolvated halide anion of this type would be easiest for chloride, less facile for bromide, the larger size of iodide and perchlorate precluding their being accommodated above or below the central aperture.

Rationalisation of the observations is possible if we consider interaction between the electrolyte anion and $H_2P^{\cdot-}$ to form a complex, which we designate $(H_2P \cdot an)^{2-}$ (noting that this may not reflect accurately the formula since for electrostatic reasons other species would almost certainly have to be involved) and the existence of two parallel reduction pathways

$$\begin{tikzcd}
 & H_2P^{\cdot-} \arrow[r] & H_2P^{2-} & \text{(A)} \\
H_2P \arrow[ur, "E^{\circ\prime}(A)"] \arrow[dr, "E^{\circ\prime}(B)"'] & & & \\
 & (H_2P \cdot an)^{2-} \arrow[r] & H_2P^{2-} & \text{(B)}
\end{tikzcd}$$

Path (A) is reversible and path (B) irreversible, its rate being a function of anion concentration, the respective formal potential values being such that $E^{\circ\prime}(\mathrm{A}) < E^{\circ\prime}(\mathrm{B, an})$. Path (B) would be important for anions Br^- and Cl^-. Above a certain anion concentration there is a progressive change from path (A) to path (B); the concentration necessary for this is less for TBAC than for TBAB.

Any contribution from the electrolyte anion desolvation energy can probably be ignored: DMF is only weakly solvating (dielectric constant 37 and Gutmann donor number 26.6 [25]). Although the detailed conformations of porphyrins in solution are largely unknown, it is unlikely that they will change very much with solvent. However, an effect of the solvent's dielectric constant on the solvation energy for mononegative ion formation has been noted, resulting in a positive shift of $E_{1/2}(1)$ [26]: for TPP on changing from $\mathrm{CH_2Cl_2}$ ($\epsilon = 9$) to dimethylsulphoxide ($\epsilon = 46$), at constant supporting electrolyte concentration, the $E_{1/2}(1)$ values were shifted from -1.20 to -1.03 V vs. SCE. In this connection we note that the presence of an anion next to the porphyrin ring would alter the local dielectric constant.

The reason as to why, with respect to behaviour in perchlorate media, the electrochemical properties vary more in halide electrolytes for TPrP than for TPP is probably linked to the effect of the anion on the porphyrin macrocycle. Since TPrP has lower electron density than TPP we can expect a greater interaction.

The lack of a composite first reduction wave on the second and successive cycles of the cyclic voltammograms and in successive RDE voltammograms must involve blocking of the electrode surface by adsorption of the product. On the first cycle it seems clear that path (B) leads to a product that is more easily adsorbed, confirmed by the RDE results.

CONCLUSIONS

Meso-tetraalkylporphyrins and *meso*-tetraphenylporphyrin may be conveniently characterised in TBAP + DMF with a glassy carbon electrode, and have an electrochemical behaviour similar to the parent porphyrin. The identity of the anion of the added electrolyte has a marked influence on the electrochemical reduction, a suggested explanation of which is based on electrolyte anion size and consequent differences in interaction with the porphyrin macrocycle facilitating a parallel, irreversible reduction pathway.

ACKNOWLEDGEMENTS

We thank Prof. A.d'A. Rocha Gonçalves and Miss M.M. Pereira for the porphyrins used in this work.

REFERENCES

1 D. Dolphin (Ed.), The Porphyrins, Academic Press, New York, 1978.
2 K.M. Smith (Ed.), Porphyrins and Metalloporphyrins, Elsevier, New York, 1975.

3 J.H. Fuhrhop, Angew. Chem. Int. Ed. Engl., 13 (1974) 321.

4 H. Behret, W. Clauberg and G. Sandstede, Ber. Bunsenges. Phys. Chem., 83 (1979) 139.

5 H.Y. Liu, M.J. Weaver, C.-B. Wang and C.K. Chang, J. Electroanal. Chem., 145 (1983) 439.

6 J.C. Lennox and R.W. Murray, J. Electroanal. Chem., 78 (1977) 395; J. Am. Chem. Soc., 100 (1978) 3710; R.D. Rocklin and R.W. Murray, J. Electroanal. Chem., 100 (1979) 271.

7 H. Yoneyama, H. Shiota and H. Tamura, J. Electroanal. Chem., 159 (1983) 361.

8 E.S. Takeuchi and R.W. Murray, J. Electroanal. Chem., 188 (1985) 49.

9 D.W. Clack and N.S. Hush, J. Am. Chem. Soc., 87 (1965) 4238.

10 A. Wolberg and J. Manassen, J. Am. Chem. Soc., 92 (1970) 2982.

11 R.H. Felton and H. Linschitz, J. Am. Chem. Soc., 88 (1966) 1113.

12 G. Peychal-Heiling and G.S. Wilson, Anal. Chem., 43 (1971) 550.

13 P. Worthington, P. Hambright, R.F.X. Williams, J. Reid, C. Burnham, A. Shamim, J. Turay, D.M. Bell, R. Kirkland, R.G. Little, N. Datta-Gupta and U. Eisner, J. Inorg. Biochem., 12 (1980) 281.

14 P. Worthington, P. Hambright, R.F.X. Williams, M.R. Feldman, K.M. Smith and K.C. Langry, Inorg. Nucl. Chem. Lett., 16 (1980) 441.

15 A. Stanienda and G. Biebl, Z. Phys. Chem., 52 (1967) 254.

16 A.M. d'A. Rocha Gonçalves and M.M. Pereira, J. Heterocycl. Chem., 22 (1985) 931.

17 H.O. House, E. Feng and N.P. Peet, J. Org. Chem., 36 (1971) 2371.

18 C.K. Mann in A.J. Bard (Ed.), Electroanalytical Chemistry, Vol. 3, Marcel Dekker, New York, 1969, p. 76.

19 A.J. Bard and L.R. Faulkner, Electrochemical Methods. Fundamentals and Applications, Wiley, New York, 1980, Ch. 13.

20 D.L. Maricle and W.G. Hodgson, Anal. Chem., 37 (1965) 1562.

21 M. Stulikova, J. Electroanal. Chem., 55 (1974) 23.

22 E.B. Fleischer, Acc. Chem. Res., 3 (1970) 105.

23 R.C. Weast (Ed.), CRC Handbook of Chemistry and Physics, 64th ed., CRC Press, Boca Raton, FL, 1983, p. F-170.

24 E.B. Fleischer and A.L. Stone, J. Chem. Soc. Chem. Commun., (1967) 332.

25 Y. Marcus, J. Sol. Chem., 13 (1984) 599.

26 K.M. Kadish and M.M. Morrison, J. Am. Chem. Soc., 98 (1976) 3326.